

Microfluidic based contactless dielectrophoretic device: modeling and analysis

S. Minnikanti, D. R. Reyes, R.C. Aguilar, J.J. Pancrazio, M. Gaitan, and N. Peixoto, *Member, IEEE*

Abstract—While there have been many attempts at patterning cells onto substrates, a reliable method for trapping cell clusters and forming cell arrays in a predefined geometry remains to be demonstrated. We intend to develop a multielectrode array platform to initially trap cells via dielectrophoresis (DEP) and to later measure their electrical activity. As a first step toward that objective, here we present an interdigitated microfabricated comb structure. We designed an optimal insulation layer via finite element modeling for maximum dielectrophoretic field strength in solution and minimal cell damage. The microfabricated structure was combined with a microfluidic channel to vertically constrain cell position. With the objective of capturing cells onto the substrate, we here show that there is an optimal thickness of dielectric which limits electrolysis in solution and still allows for sufficient dielectrophoretic force on the cells to pull them onto the surface.

I. INTRODUCTION

Despite recent advances in cell patterning and *in vitro* cellular networks, a reliable, efficient, and fast method for cell positioning and monitoring remains to be demonstrated. Our objective is to design a platform for multicell trapping and positioning which allows for other cell-based studies. Previously proposed methods for cell positioning and trapping range from optical tweezers [1], [2] to micromanipulation [3] and microfabricated devices [4] with wells and overhanging structures [5]. One of these techniques, dielectrophoresis (DEP), has been successfully used to manipulate, trap, and also separate biological cells via high gradient electric fields [6], [7]. DEP forces are experienced by particles in suspension under the influence of non-uniform electric fields [8].

The DEP force can move a particle towards areas of high-field (positive DEP) or low-field strength (negative DEP), depending on the difference of electrical properties between the particles and the suspending medium [9]. The electrical properties are dependent on the frequency of the applied signals [9]. For manipulating cells suspended in media, non-uniform electric fields are generated via patterned microelectrodes using micro-electro-mechanical-systems (MEMS) based fabrication techniques [10]. To further improve the yield of this technique, a microchannel is

usually fabricated in order to serve as conduit to the solution where the cells are dispersed.

In this study we investigated the contact between the electrodes and the medium. This is a critical when dealing with biological cells due to (1) possible hydrolysis when the electric potential in solution surpasses the water window; (2) joule heating of the solution due to the electric field applied increases with amplitude.

When an AC field is applied across two electrodes, there will be a non uniform electric field generated in the medium [11]. The absence of contact between the electrodes and the cell media in the microchannel reduces the issues associated with traditional DEP approaches [11], however, a thick dielectric would trap the electric field and not allow for any DEP process to take place. Therefore, we investigated the how insulating layer thickness impacts the trapping electric fields and forces.

We performed finite element analysis to simulate the electric field distribution and the DEP forces acting at a nano and microscale for an interdigitated electrode configuration. Keeping the electrode configuration constant, the insulation layer was varied in each model to estimate the electric field and DEP forces in each case.

II. METHODS

A. Theory

The DEP force acting on a spherical particle is as follows:

$$F_{dep} = 2\pi\epsilon_m R^3 Re[f_{CM}] \nabla |E_{rms}|^2 \quad (1)$$

where ϵ_m is the permittivity of the suspending medium, R is the radius of the particle, $\nabla |E_{rms}|^2$ is the local electric field gradient. $Re[f_{CM}]$ is the real part of the complex factor f_{CM} (Clausius-Mossotti) which is represented by equation:

$$f_{CM} = \frac{\epsilon_p^* - \epsilon_m^*}{\epsilon_p^* + 2\epsilon_m^*} \quad (2)$$

Where ϵ_p^* and ϵ_m^* are complex permittivity of the particle and media defined as follows:

$$\epsilon^* = \epsilon - j \frac{\sigma}{\omega} \quad (3)$$

ϵ is the permittivity, σ is the conductivity, $j^2 = -1$, and ω is the angular frequency. The DEP force experienced by the particle in media is dependent on the electrical properties of both the particle and the media.

Manuscript received April 1st, 2010.

S.M, J.J. P., and N.P. are with the Electrical and Computer Engineering Dept. of George Mason University, Fairfax VA. tel. 703 993 1567 fax. 206 600 4261 ({smnikanti, jpancraz, npeixoto}@gmu.edu)

R.C.A. is with the Biological Sciences Dept of Purdue University, West Lafayette, IN.

D. H.-R. and M.G. are with the National Institute of Standards and Technology, Gaithersburg MD.

B. Microfluidic device fabrication

A sacrificial layer of photoresist was used to pattern gold electrodes evaporated onto glass onto a chromium adhesion layer (10 nm). The ITO (Indium Tin Oxide) electrodes, 20 nm high, 10 μm wide with 10 μm inter-electrode spacing, were insulated with polystyrene (PS) (80 nm thick) in the cell trapping regions. A polydimethylsiloxane (PDMS) mold fabricated by standard methods was attached conformally to this substrate to act as a microfluidic channel (250 μm wide, 30 μm deep) perpendicular to the microelectrodes. Access holes punched in the PDMS allowed fluidic access to the microchannel, and NanoPort assemblies enabled fluidic control via syringe pumps.

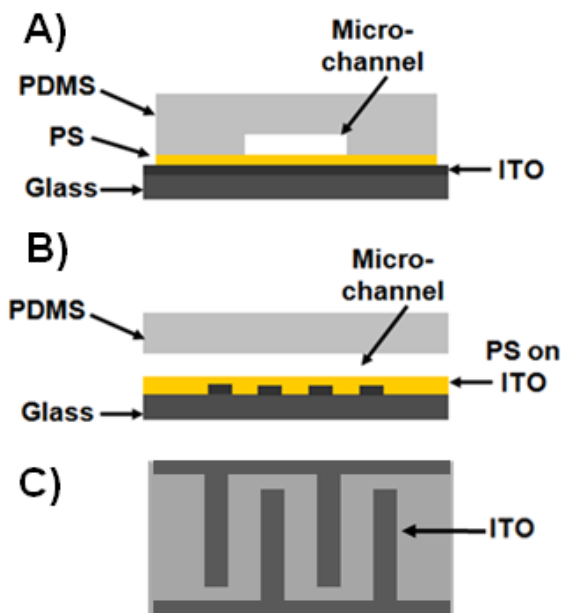


Fig. 1. Cross section (A), a side view (B), and top view (C) respectively, of the DEP device, which consists of an interdigitated array of ITO electrodes on a glass substrate. The ITO electrodes are passivated by spin coating a thin layer (~ 80 nm) of PS. A PDMS microchannel is aligned perpendicular to the ITO electrodes and reversibly bound to the passivated substrate.

C. Modelling

2D finite element models were created of the fabricated microfluidic device using AC/DC module in COMSOL Multiphysics 3.5 (Burlington, MA). The 2D model geometry can be seen in Fig. 2. In these simulations, ITO electrodes, 10 μm wide by 20 nm thick, with 10 μm inter-electrode spacing are placed on top of a glass substrate (40 μm wide by 10 μm thick). The electrodes, as in the microfabricated device, are insulated with a layer of PS (80 nm thick) and a microfluidic channel 30 μm thick lies on top of the insulation. The electrodes are thus not directly in contact with the microchannel. The outer boundaries of model are defined as insulating. The upper boundaries for the electrodes are chosen such that one is driven by an AC signal of 10 V peak-to-peak at 10 MHz (left in Fig. 2) and other is grounded (right in Fig. 2). The continuity conditions are used for the rest of the interior boundaries. The electric field distribution and its gradient were calculated by solving

for the potential distribution using Laplace equation. Values for the electrical conductivity and permittivity for different layers of the structure and media that were used in this numerical modeling are given in Table 1. The electric field around the electrodes is first solved in the AC/DC module. Then the gradient of the electric field is evaluated to determine the DEP forces acting within the microfluidic channel. The electric field gradient is then computed in the x and y directions. Two other models were also evaluated: one without the polystyrene insulation and other having a 2 μm thick insulation on top of the electrodes.

TABLE I
ELECTRICAL PROPERTIES OF THE MATERIALS AND FLUIDS

Materials	Electrical conductivity (S/m)	Relative Electrical Permittivity
Glass	10^{-12}	4.6
ITO	10^6	10
Polystyrene	10^{-14}	2.4
Sucrose Cell	0.1	80

III. RESULTS

Fig. 2 shows the induced electric field distribution inside the microfluidic channel filled with sucrose with a conductivity of 0.1 S/m. The electric field is enhanced at the edges of the electrode and is greatest at electrode edges between the microelectrodes. The electric field value near the outer electrode edges is of the order of 0.6 V/ μm . The DEP force was calculated by creating a subdomain expression defined as in equation 1 in both x and y direction. The solid arrows in Fig. 2 indicate the direction of DEP force, which is strongly directed towards the two electrodes.

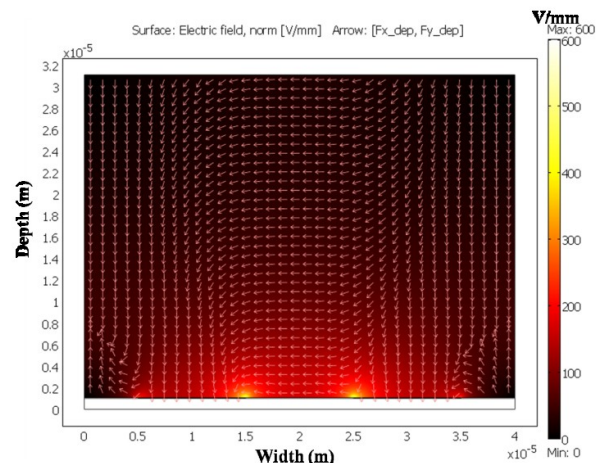


Fig. 2. Surface plots of simulated electric field distribution in the microfluidic channel and arrow plot of the normalized DEP force acting in the channel, above the two electrodes. The electrodes are coated with a thin layer (70 nm) of PS. The maxima of the electric field intensity are at the edges of the electrodes. Maximum electric field in this case is 0.6 V/ μm .

The frequency used for stimulation (10 MHz) lead to positive DEP force. Thus the cells will be attracted towards region of higher electric field intensity. The electric field

generated in the absence of the PS layer (Fig. 3) is extremely high ($7 \text{ V}/\mu\text{m}$). The color scale for Fig. 3 is adjusted to the maxima of Fig. 2, for a better comparison between the two models. As expected, the direction of DEP force was strongly directed towards the two electrodes so long as the particle is located above the two electrodes.

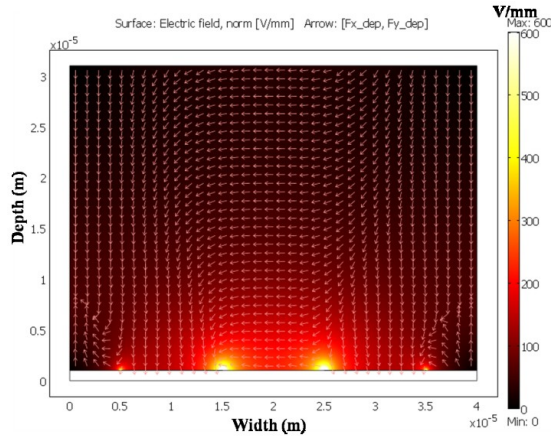


Fig. 3. Surface plots of simulated electric field distribution in the microchannel. Arrows indicate the normalized DEP force acting in the microchannel. The electrodes are not insulated with PS. The peak of the electric field is at the inner edges of the electrodes. The direction of DEP force is towards the electrodes. However, the electric field generated is higher compared to Fig. 2.

However, by increasing the PS thickness to $2 \mu\text{m}$ the maximum electric field estimated falls steeply, to $0.032 \text{ V}/\mu\text{m}$ (Fig. 4). Under this condition, the direction of DEP force was strongly directed towards the two electrodes but will not be sufficient to trap the cells.

Interestingly, the profile of the DEP force changes with the insulation layer. The y and x directions of the DEP force contribute differently to its normalized profile. As Fig. 5 shows, the uninsulated case (upper curve) shows a high peak in the y direction (vertically) on the outer edge of the electrodes. However, with a thin insulating layer (80 nm) the maximal force is seen at the inner edge of the electrodes. As expected, with a thick polystyrene layer there is almost no electric field in the solution, and thus the force exerted onto particles in suspension are negligible

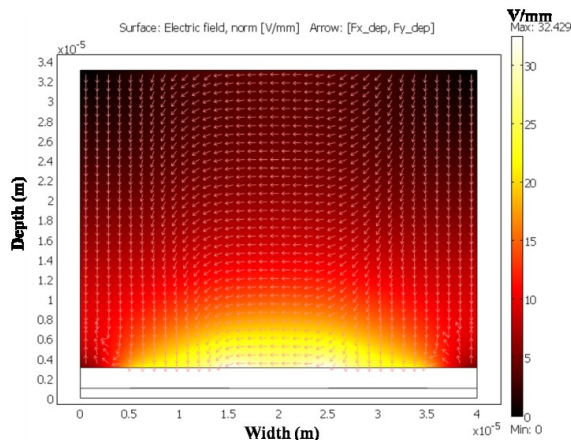


Fig. 4. Surface plots of simulated electric field distribution in the microchannel. Arrows indicate the normalized DEP force acting in the microchannel. The electrodes are coated a thick layer ($2 \mu\text{m}$) of PS. The

maximum of the electric field intensity is at the edges of the electrodes. The direction of DEP force is towards the electrodes.

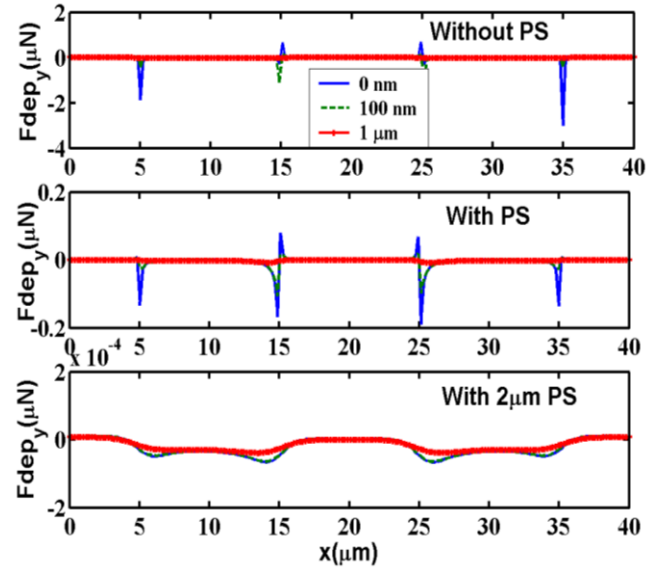


Fig. 5. DEP force (y direction) plotted as a function of x for different depths in the microchannel moving away from the electrode surface for models with and without the polystyrene (PS) coating on top of the ITO electrodes.

IV. CONCLUSION

Our results show that the electric field generated with a thin insulated layer is almost 10 times lower in comparison to a non-insulated channel. However, previous experimental results from our group [12] have shown that the fields induced with insulation on top of the electrodes are sufficient to trap the biological cells on electrode sites.

The forces operating on a particle in a microfluidic channel under the influence of a non uniform electric field are multi-faceted. These include electro-thermal and hydrodynamic forces [13], [10]. Future simulations will encompass fluid dynamics (drag forces) and electro-thermal influence (joule heating) along with the moving mesh feature to determine the effect of drag forces on the cells dispersed in the sucrose media. With these additional simulation features, we will be able to improve predictions for cell deposition under the influence of the combined electro-thermal, drag, and dielectrophoretic forces.

ACKNOWLEDGMENT

The first author thanks the Cosmos Club of Washington (Washington, DC) for financial support.

REFERENCES

- [1] X.C. Yao and A. Castro, "Optical trapping microfabrication with electrophoretically delivered particles inside glass capillaries," *Optics letters*, vol. 28, 2003, pp. 1335–1337.
- [2] H. Hsu, A.T. Ohta, P. Chiou, A. Jamshidi, S.L. Neale, and M.C. Wu, "Phototransistor-based optoelectronic tweezers for dynamic cell manipulation in cell culture media," *Lab on a Chip*, vol. 10, 2010, pp. 165–172.
- [3] N. Ashida, S. Ishii, S. Hayano, K. Tago, T. Tsuji, Y. Yoshimura, S.

- Otsuka, and K. Senoo, "Isolation of functional single cells from environments using a micromanipulator: application to study denitrifying bacteria," *Applied Microbiology and Biotechnology*, vol. 85, Jan. 2010, pp. 1211-1217.
- [4] C. Moraes, J.H. Chen, Y. Sun, and C.A. Simmons, "Microfabricated arrays for high-throughput screening of cellular response to cyclic substrate deformation," *Lab on a Chip*, vol. 10, 2010, pp. 227-234.
- [5] S.M. Potter, J. Pine, and S.E. Fraser, "Neural Transplant Staining with DiI and Vital Imaging by 2-Photon Laser-Scanning Microscopy," *Scanning microscopy. Supplement*, vol. 10, 1996, pp. 189-199.
- [6] U. Kim, C. Shu, K.Y. Dane, P.S. Daugherty, J.Y.J. Wang, and H.T. Soh, "Selection of mammalian cells based on their cell-cycle phase using dielectrophoresis," *Proceedings of the National Academy of Sciences*, vol. 104, Dec. 2007, pp. 20708-20712.
- [7] S. Burgarella, S. Merlo, B. Dell'Anna, G. Zarola, and M. Bianchessi, "A modular micro-fluidic platform for cells handling by dielectrophoresis," *Microelectronic Engineering*, vol. In Press, Corrected Proof.
- [8] H.A. Pohl, *Dielectrophoresis: the behavior of neutral matter in nonuniform electric fields*, Cambridge University Press Cambridge, 1978.
- [9] J. Voldman, "Electrical forces for microscale cell manipulation," *Annual Review of Biomedical Engineering*, vol. 8, 2006, pp. 425-454.
- [10] M. Lian, N. Islam, and J. Wu, "AC electrothermal manipulation of conductive fluids and particles for lab-chip applications," *Nanobiotechnology, IET*, vol. 1, 2007, pp. 36-43.
- [11] H. Shafiee, J.L. Caldwell, M.B. Sano, and R.V. Davalos, "Contactless dielectrophoresis: a new technique for cell manipulation," *Biomedical Microdevices*, vol. 11, 2009, pp. 997-1006.
- [12] S.P. Forry, D.R. Reyes, M. Gaitan, and L.E. Locascio, "Cellular Immobilization within Microfluidic Microenvironments: Dielectrophoresis with Polyelectrolyte Multilayers," *Journal of the American Chemical Society*, vol. 128, Oct. 2006, pp. 13678-13679.
- [13] D. Wang, M. Sigurdson, and C.D. Meinhart, "Experimental analysis of particle and fluid motion in ac electrokinetics," *Experiments in Fluids*, vol. 38, Jan. 2005, pp. 1-10.